

Inhibition of Photocatalyst-Assisted Electron Transfer at ITIES Under Simulated Solar Irradiation-the Role of Supporting Electrolyte

Edwin Avella,^[a] Andrea Folli,^[b] and Angel Cuesta^{*[a]}

Photocatalyst-assisted charge transfer at the interface between two immiscible electrolyte solutions (ITIES) has been previously proven. However, its practical application requires information on its performance under solar irradiation. We investigated photocatalyst-assisted oxidation of water at ITIES under solar irradiation using TCNQ 7,7,8,8-Tetracyanoquinodimethane (TCNQ) as electron scavenger and bis(triphenylphosphoranylidene) ammonium tetrakis(4-chlorophenyl)borate (BTPPA-TPBCl) as organic phase electrolyte. No enhancement of water oxidation after assembling photocatalyst nanoparticles at the ITIES was observed. Photocurrents with photocatalyst were similar to those without but in the presence of TCNQ. Photocurrents observed both with and without photocatalyst are shown to be due to photogeneration

of TCNQ^{•-}, either by reaction with the organic electrolyte or by interfacial oxidation of water. The former dominates at positive potentials and results in a positive photocurrent due to transfer of TCNQ^{•-} across the ITIES. The latter dominates at negative potentials and results in a negative photocurrent. Electron paramagnetic resonance (EPR) detected TCNQ^{•-} and revealed its stabilisation by formation of an adduct with BTPPA⁺, which must contribute to making the photoactivity of TCNQ the dominant process even with photocatalyst. These findings highlight the necessity of research on alternative suitable electron scavenger-supporting electrolyte combinations for implementing ITIES in the photoelectrocatalytic conversion of solar energy.

Introduction

Hydrogen production has been the focus of research over the last decades as one of the most important alternatives to fossil fuels due to its high heating value of 141.8 MJ kg⁻¹ and the absence of greenhouse gas emissions after combustion.^[1] Nowadays, hydrogen is mainly produced from steam methane reforming (SMR). Despite the efforts to increase the efficiency of carbon capture units (CCU) coupled in tandem with SMR, enhancing the efficiency of CCU by more than 90% increases the energy consumption of this type of systems, which directly impacts the cost of hydrogen production.^[2]

An exciting alternative for fossil fuel-based hydrogen production is photocatalytic water-splitting using solar light. Photocatalysis has the advantage that no additional energy must be supplied in the form of heat (as in SMR) or electricity

to the system (as in conventional water-splitting electrolyzers), as the photons absorbed by a semiconductor will provide the Gibbs energy required to perform this reaction. Photocatalytic hydrogen production has been investigated since the work of Fujishima and Honda,^[3] who reported for the first time photoelectrochemical H₂ production using TiO₂ as the photocathode. Since then, intensive research has been performed to use direct solar light as an energy source for photocatalytic applications.^[4–8]

One of the limitations to the implementation of photocatalytic water splitting is the band gap of suitable photoactive materials. The most widely used TiO₂ (anatase) possesses a band gap of approximately 3.2 eV, well into the near-UV light region, which accounts for only 4% of the solar spectrum.^[9,10] Additionally, photocatalytic activity is limited by the high recombination rate of photogenerated electron-hole pairs. Modifications to prevent the recombination rate, such as nanoparticle deposition, 3D structure design and doping of the photocatalyst, have been attempted.^[11–18] Although these modifications have demonstrated to be efficient in increasing the photocatalytic activity, the additional steps required in the synthesis contribute to preventing commercial application.


Additionally, in photocatalytic water splitting, the redox processes (HER and OER), are typically performed in the same solution.^[19,20] In this type of setup, photogenerated H₂ and O₂ can recombine, reducing the hydrogen production yield^[15] and creating the risk of explosion. A setup where the photocatalytic HER and OER occur in separate solutions is therefore much more convenient. The interface between two immiscible electrolyte solutions (ITIES) is an excellent alternative in this


[a] E. Avella, A. Cuesta

Advanced Centre for Energy and Sustainability (ACES), School of Natural and Computing Sciences, University of Aberdeen, AB24 3UE Aberdeen, Scotland, UK
E-mail: angel.cuestaciscar@abdn.ac.uk

[b] A. Folli

Cardiff Catalysis Institute, Net Zero Innovation Institute, School of Chemistry, Cardiff University, Translational Research Hub - Maindy Road, CF24 4HF Cardiff, UK

 Supporting information for this article is available on the WWW under <https://doi.org/10.1002/celec.202400333>

 © 2024 The Authors. ChemElectroChem published by Wiley-VCH GmbH. This is an open access article under the terms of the Creative Commons Attribution License, which permits use, distribution and reproduction in any medium, provided the original work is properly cited.

regard, as it can provide a frame where the redox reactions can occur separately and charge transfer across the liquid-liquid interface can be controlled by varying the Galvani potential between the solutions.^[21]

The pioneering work of Volkov, Kandelaki and collaborators^[22–25] demonstrated the feasibility of water oxidation at the ITIES. In their work, chlorophyll was adsorbed at the octane/water interface, facilitating light absorption and water photooxidation. They proposed a four-electron mechanism involving a hydrated chlorophyll oligomer that enabled the photo-assisted oxygen evolution.

Photo-induced charge transfer at the ITIES was also shown by Marecek et al.^[26] using water/1,2-DCE, and water/benzonitrile interfaces. This was achieved by dissolving methyl viologen in the aqueous phase and Ru(bpy)₃²⁺ in the organic phase. Additionally, Thompson et al.^[27] also described successful photo-assisted electron transfer across a liquid-liquid interface using the Ru(bpy)₃²⁺/C₇V²⁺ system. In their experiment, ion transfer was inhibited due to changes in the hydrophobicity of the photoproducts. In a subsequent study, Brown et al.^[28] successfully demonstrated photoinitiated electron transfer using Ru(bpy)₃²⁺ at a water/1,2-DCE interface with TCNQ in the organic phase. They showed that the products of this transfer stayed in their respective phases, preventing back electron transfer, which is crucial for photoelectrochemical energy conversion.

Samec et al.^[29,30] have analysed the photo-assisted ion transfer at the ITIES. Photocurrents due to the interfacial transfer of long-lived photoproducted species generated from the supporting electrolytes were observed upon irradiation of the ITIES. Please note that no electron quencher such as, e.g., TCNQ, was used in this work.

More recently, Girault and co-workers^[31–37] have demonstrated in a series of papers the photo-assisted electron transfer across ITIES from ferrocene derivatives in the organic phase to photosensitive porphyrins in the aqueous phase. Later, the same group^[38–40] as well as Plana and Fermin^[41] have demonstrated the possibility of assembling a photocatalyst at the ITIES by controlling the Galvani potential between the adjacent phases. These photocatalyst layers can transfer the photo-generated electron and hole to opposite sides of the ITIES to generate either hydrogen or oxygen on the aqueous side of the interface, while a suitable hole or electron scavenger in the organic phase captures the charge carrier left behind. Plana et al.^[42] have also shown that spontaneously deposited mesoporous photocatalyst films at the ITIES can reach high photon-to-current efficiency. This work has demonstrated the feasibility of photocatalytic-assisted electron transfer aided by either an electron or a hole scavenger in the organic phase. These photocatalyst assisted electron transfer experiments,^[38–42] however, were performed using monochromatic UV light. Therefore, evidence of the feasibility of photo-assisted electron transfer by nanoparticle films at the ITIES under solar irradiation is necessary. In this contribution, we show that, under solar irradiation, the possibly most common electron scavenger in the organic phase, 7,7,8,8-Tetracyanoquinodimethane (Figure 1b), has a higher photoactivity than common photocatalysts

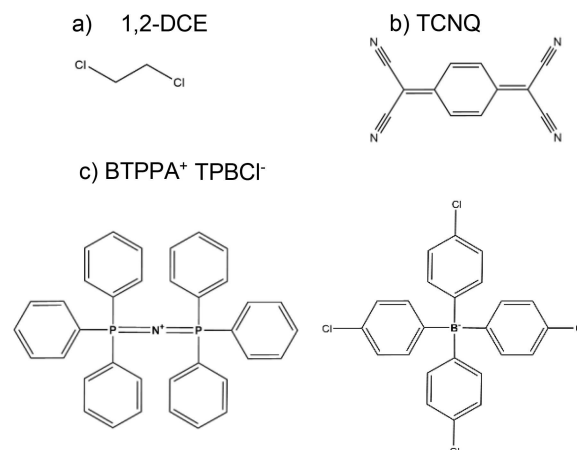


Figure 1. Chemical species present in the organic phase a) 1,2-dichloroethane (1,2-DCE) as solvent. b) TCNQ 7,7,8,8-Tetracyanoquinodimethane (TCNQ) as electron scavenger. c) bis(triphenylphosphoranylidene) ammonium tetrakis(4-chlorophenyl)borate (BTPPA⁺ TPBCl⁻) as supporting electrolyte.

like TiO₂ or WO₃. We also show that when dissolved in 1,2-dichloroethane (Figure 1a) and in the presence of the also possibly most common organic-electrolyte, bis(triphenylphosphoranylidene) ammonium tetrakis(4-chlorophenyl)borate (Figure 1c), solar irradiation results in the reduction of TCNQ to the corresponding radical anion even in the absence of an ITIES and/or a photocatalyst. Finally, we demonstrate the photo-formation, under visible light, of an adduct [BTPPA⁺-TCNQ^{•-}] which harvests most of the irradiation inhibiting the photocatalytic response of the photocatalyst assembled at the ITIES. These results call for the search of different suitable electron scavenger-supporting electrolyte pairs for practical applications of ITIES for photoelectrocatalytic conversion of solar energy. We mention in passing that no unexpected behaviour was observed when reducing water to hydrogen with solar irradiation using a variety of photocatalysts (TiO₂, CuO, SrTiO₃) and ferrocene dissolved in a DCE solution of BTPPA-TPBCl as the hole scavenger.

Results and Discussion

TCNQ's photoactivity was observed when attempting to photo-oxidise water to oxygen by assembling a suitable photocatalyst at the interface between a pH 11 aqueous solution and a TCNQ-containing solution of BTPPATPBCl in DCE. The selection of pH is due to the shift in the CB potential of the nanoparticles assembled at the interface towards negative potential at higher pH values, which enhances the electron transference towards the TCNQ.^[38] We had chosen WO₃ (<100 nm particles) and TiO₂ (anatase, 5 nm particles) as model photocatalysts, because we expected their band gaps (3.2 eV for TiO₂ (anatase) and 2.46 eV for WO₃, see Figure S1) to be different enough as to result in different rates of oxygen production when illuminating the interface.

The effect of the deposition of the photocatalyst at the ITIES and of the transfer of photogenerated charge carriers across the ITIES was analysed using a 3-compartment cell (Figure 2a). The composition of the cell is schematically described in Figure 2b, where σ represents the interface studied. The geometric area of σ in the cell used was 1.54 cm^2 . A coalescence method was used to deposit photocatalyst nanoparticles at the ITIES.^[42] Two Ag/AgCl (KCl_{sat}) reference electrodes, one in the aqueous phase and the other in the organic electrolyte, were used to control the Galvani potential difference across the liquid-liquid interface. The potential difference measured between these two reference electrodes was corrected using the formal transfer potential of tetramethylammonium ($\phi^w - \phi^o = \Delta\phi_o^w \phi^o = 0.160 \text{ V}$).^[36] The catalyst dosage in the organic phase was calculated to result in the deposit of approximately five photocatalyst layers at the ITIES. This estimation was done based on the particle size of the catalyst, considering the migration of all nanoparticles to the interface but omitting electrostatic interactions and particle coalescence.

Cyclic voltammograms (CVs) of the water/1,2-dichloroethane (DCE) interface in the presence of TCNQ in the organic phase both without photocatalyst and with layers of TiO_2 and WO_3 spontaneously assembled at the interface are shown in Figure 2c. The positive potential limit of the potential window is determined by the transfer of Li^+ from the aqueous to the organic phase, whereas transfer of Cl^- determines the negative potential limit. The CV of the ITIES in the absence of assembled photocatalyst and in the absence of TCNQ in the organic phase shows a capacitive current lower than $0.5 \mu\text{A cm}^{-2}$ (see Figure S2), corresponding to a capacitance $< 10 \mu\text{F cm}^{-2}$, which is consistent with the value of ca. $1 \mu\text{F cm}^{-2}$ obtained by EIS after fitting to an RC circuit. This suggests that the ITIES behaves as a

sharp interface in the absence of a photocatalyst. A clear increase of the capacitive current is observed after deposition of TiO_2 ($120 \mu\text{A cm}^{-2}$) and WO_3 ($60 \mu\text{A cm}^{-2}$) at the ITIES. This increase can be attributed to an increase in the roughness, and therefore the real surface area, of the interface, as supported by the fact that the smaller TiO_2 nanoparticles (5 nm) lead to a larger increase of the interfacial capacitance than the WO_3 particles ($< 100 \text{ nm}$).

All the CVs in Figure 2c contain a voltammetric wave centred around 0.21 V , which we attribute to the reversible transfer of $\text{TCNQ}^{\bullet-}$ across the interface. The EPR results discussed below suggest the presence of $\text{TCNQ}^{\bullet-}$ traces in our TCNQ-containing DCE solutions, which explains the presence of this wave in the CVs of Figure 2c.

Photocurrent transients resulting from irradiation with simulated solar light of the ITIES are shown in Figure 3, without any photocatalyst (Figure 3a), with WO_3 assembled at the interface (Figure 3b) and with TiO_2 assembled at the interface (Figure 3c). Photocurrents are only observed when the electron scavenger TCNQ is present in the organic phase, even if the photocatalyst is not present. The values of the conduction band potentials of TiO_2 and WO_3 are -0.11 ^[38] and 0.5 ^[43] V vs NHE, respectively, at pH 0. Under our experimental conditions (pH 11), the estimated conduction band potentials are -0.759 (TiO_2) and -0.149 V (WO_3).^[38] The redox potential of TCNQ in 1,2-DCE is 0.29 V vs SHE.^[38] Therefore, photo-assisted electron transfer from the photocatalyst's conduction band to the TCNQ in the organic phase should be possible under our experimental conditions. Therefore, a sharp increase in the characteristic photocurrents is expected when a photocatalyst is present in the system. However, the experimental results show that both the magnitude and the shape of the photocurrent transients

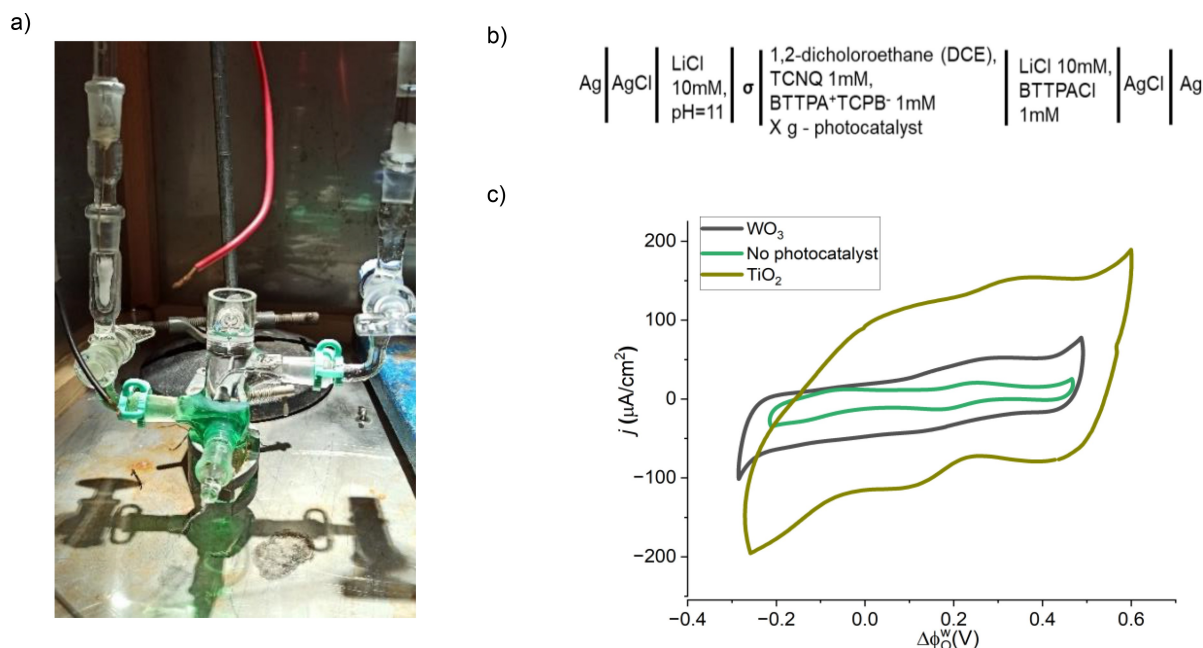


Figure 2. a) 3-compartment cell used in the photo-electrocatalytic tests; b) Schematic representation of the electrochemical cell; c) Cyclic voltammograms at 50 mV s^{-1} of the ITIES in the presence of TCNQ dissolved in the organic phase in the absence of a photocatalyst layer (red line) and with either WO_3 (black) or TiO_2 (green) assembled at the ITIES.

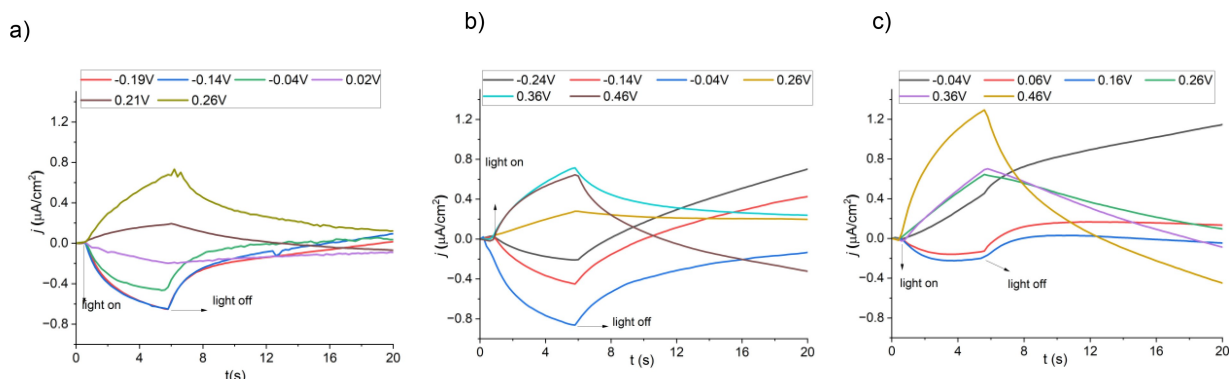
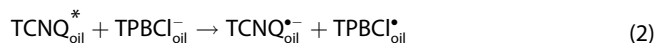


Figure 3. Photocurrent transient responses when illuminating with a solar simulator the ITIES between a 10 mM LiCl aqueous solution and a 10 mM BTPPA⁺TPBCl⁻ + 1 mM TCNQ solution in DCE in the absence of photocatalyst (a), in the presence of five layer of WO₃ assembled at the ITIES (b) and in the presence of 5 layers of TiO₂ assembled at the ITIES (c).

are similar in the presence and in the absence of a photocatalyst layer assembled at the ITIES, suggesting that the photoactivity observed comes from TCNQ, and not from either WO₃ or TiO₂. Additionally, a change of colour from pale yellow to an intense green was observed after irradiation, suggesting that TCNQ undergoes a photoinduced reaction under the experimental conditions.

Positive photocurrents are registered at $\Delta_o^w \phi > 0.21$ V, resulting in transients suggesting a diffusion-controlled process (Figure 3a). Similar positive photocurrents were reported by Kotov and Kuzmin^[44,45] when irradiating an ITIES formed by an aqueous NaCl solution and a DCE solution containing tetrabutylammonium tetrphenylborate as the electrolyte and different quinones (either benzo-, tolu-, duro- or anthraquinone) with light corresponding to the absorption maximum of the specific quinone used (313 nm for benzo- and toluquinone, 365 nm for duro- and anthraquinone). The photocurrent was attributed to the transfer across the ITIES of the quinone anion radical obtained after oxidation in the organic phase of tetrphenylborate by the photogenerated triplet of the excited state of the quinone. Following Kotov and Kuzmin,^[44,45] we suggest that the positive photocurrents observed at $\Delta_o^w \phi > 0.21$ V are the consequence of Reactions 1 to 3.



This interpretation is supported by the fact that the positive photocurrents appear at potentials more positive than that corresponding to the transfer process observed in the CVs in the presence of TCNQ (Figure 2), which we have precisely attributed to the presence of traces of TCNQ^{•-} in the organic phase and the transfer of TCNQ^{•-} across the ITIES. Interfacial transfer of TCNQ^{•-} has also been observed by Vishwanath *et al.* in a 3-phase junction in an aprotic medium.^[46]

Negative currents are observed instead at $\Delta_o^w \phi < 0.16$ V (Figure 3). A negative photocurrent implies either the transfer

of an electron or anion from the aqueous phase to the organic phase, or the transference of a cation from the organic phase to the aqueous phase. The only anion present in the aqueous phase is chloride, and it is only transferred to the organic phase when the positive limit of the potential window is reached. The only cation in the organic phase is BTPPA⁺, and it is not transferred to the aqueous phase within the available potential window. Therefore, the only option left for the negative photocurrent observed in the presence of TCNQ in the organic phase at $\Delta_o^w \phi < 0.16$ V is the photo-induced transfer of an electron from the aqueous to the organic phase. Given the composition of the aqueous electrolyte, this electron must come from the oxidation of either H₂O or Cl⁻, of which we consider the first option as the more likely.

Figure 3b and c show the effect of depositing five layers of WO₃ and TiO₂, respectively, at the ITIES. In both cases, positive and negative photocurrents are observed positive of 0.21 V and negative of 0.16 V, respectively, similar in magnitude and shape to those observed in the absence of a photocatalyst layer, Figure 3a. These results suggest that the photocatalyst layers are not involved in the photo-induced charge transfer processes, which remain mediated by the photoexcitation of TCNQ instead.

A TCNQ-assisted photo-induced charge transfer was not observed when either CdSe^[40] or TiO₂^[38] were assembled at the same ITIES,^[33] and TCNQ was present as an electron scavenger in the organic phase.^[31] The shape of the photocurrent transients, with an initial rapid increase followed by a plateau, was also different. In those cases, the photo-induced interfacial charge transfer was indeed mediated by the photocatalyst and not TCNQ. However, whereas radiation from a solar simulator was used by us, monochromatic UV light (325 nm with TiO₂, 454 nm with CdSe) was always used in the previously cited works. Light absorption by TCNQ to form the excited triplet was found by Khvostenko *et al.*^[47] to occur around 630 nm, which is consistent with the yellow colour of TCNQ-containing DCE solutions. Therefore, the formation of TCNQ* was not possible under their experimental conditions. It must be stressed, however, that our results are more relevant for practical applications using solar radiation.

The degradation of the electrolyte due to irradiation suggested in the preceding paragraphs is confirmed by the change in the colour of the DCE-based electrolyte from yellow to green after irradiation with solar light (Figure S3).

Electron paramagnetic resonance (EPR) was used to confirm the formation of $\text{TCNQ}^{\bullet-}$ and understand the role of the $\text{BTTPA}^+\text{TPBCl}^-$ electrolyte. Spectra of DCE solutions containing either only 1 mM TCNQ or only 10 mM $\text{BTTPA}^+\text{TPBCl}^-$, acquired using a standard EPR tube (Figure S4), did not show evidence of any radical species either before, during or after irradiation. However, when the solution contains both TCNQ and $\text{BTTPA}^+\text{TPBCl}^-$, a single resonance line (red spectrum in Figure 4, linewidth ca. 0.5 mT) immediately appeared upon irradiation with unfiltered light from a tungsten lamp, the intensity of which increased significantly and very quickly until reaching a maximum after ca. 30 minutes of irradiation time, and then started decreasing (Figure 5a and b). The overall increase in intensity was 200-fold. The decrease in intensity after the maximum results in the emergence of a clear hyperfine structure at irradiation times >4000 s (Figure 5a). This suggests

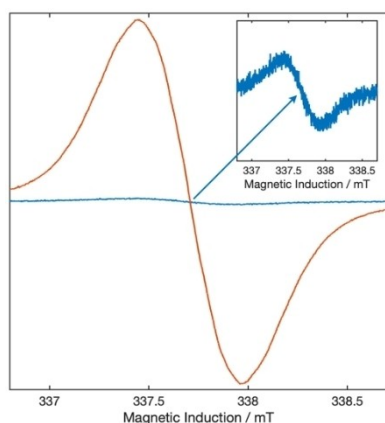


Figure 4. EPR spectra of a 1 mM TCNQ + 10 mM $\text{BTTPA}^+\text{TPBCl}^-$ solution in 1,2-DCE before irradiation (blue trace), and under UV-vis irradiation (red trace).

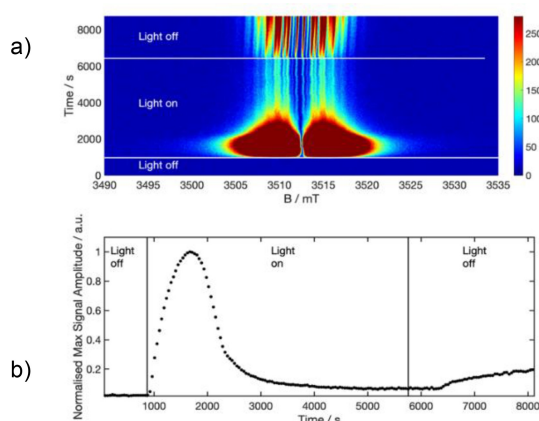


Figure 5. a) 2-D representation of the time evolution of the EPR spectrum of the same solution used in Figure 4 upon, during and after irradiation. b) Evolution of the maximum EPR signal amplitude of the absorption maximum of the EPR spectrum upon, during and after irradiation.

that, initially, a high concentration of a radical is formed with rapid kinetics and the resulting EPR spectrum is (most likely) concentration broadened (essentially causing a shorter T_2 relaxation time). As the radical is consumed (this time with a much slower kinetics), and its concentration drops, the linewidth is narrowed, and a clear hyperfine structure emerges. Interestingly, when the light is turned off, the EPR signal intensity increases again. At the moment we have no explanation for this behaviour, but we are planning experiments using other spectroscopic techniques like NMR and UV-vis, aimed at following changes in the composition of the electrolyte during and after irradiation. It is worth noting that, even before irradiating the TCNQ-containing electrolyte solution, a small signal can be observed at the same position and with the same linewidth. This suggests the presence of traces of the photo-generated radical in the solution, probably formed by exposure to natural light. This is consistent with the voltametric wave observed in CVs of our ITIES when TCNQ is present in the organic phase (see Figure 2c and the corresponding discussion).

EPR spectra were also obtained with systems containing an ITIES between an aqueous 10 mM LiCl (pH = 11) and a 1 mM TCNQ + 10 mM $\text{BTTPA}^+\text{TPBCl}^-$ solution in 1,2-DCE using a standard flat cell (Figure S5). The EPR recorded corresponds to the organic phase in a region close to the water-organic ITIES. Figure 6a shows the spectrum recorded at open circuit potential ($\Delta\phi = 0.17$ V) under irradiation. The spectrum is identical to that recorded in the pure organic phase (i.e., no ITIES) after long irradiation and after switching the light off (Figure 5a).

The simulation of the EPR spectrum in Figure 6a indicated that the photo-formed radical corresponds to $\text{TCNQ}^{\bullet-}$, with isotropic hyperfine coupling constants (hfccs) $a^{\text{H}} = 0.143$ mT (x4, accounting for the four magnetically equivalent aromatic protons of TCNQ) and $a^{\text{N}} = 0.102$ mT (x4, accounting for the four magnetically equivalent ^{14}N atoms on the nitrile moieties of TCNQ). This is in good agreement with previous reports of the electrochemical formation of $\text{TCNQ}^{\bullet-}$ by Fischer and McDowell^[48] ($a^{\text{H}} = 0.144$ mT, $a^{\text{N}} = 0.102$ mT) and Rieger *et al.*^[49] ($a^{\text{H}} = 0.157$ mT, $a^{\text{N}} = 0.110$ mT). However, our spectrum could not be fully simulated as a $\text{TCNQ}^{\bullet-}$ radical anion only. The best simulation of the experimental spectrum was achieved by computing an extra superhyperfine coupling constant to the ^{14}N nucleus of BTTPA^+ , with hfcc equal to $a^{\text{N}} = 0.029$ mT. No superhyperfine coupling to the ^{31}P atoms of the BTTPA^+ was observed. This suggests that the formation of the radical anion is favoured by the stabilising interaction with the electrolyte cation, which is in good agreement with the observation that the radical cannot be detected in only TCNQ is dissolved in DCE. DFT calculations confirmed this hypothesis as the $[\text{BTTPA}^+ \cdot \text{TCNQ}^{\bullet-}]$ adduct could be successfully geometry optimised, Figure 6b.

The detection of the $\text{TCNQ}^{\bullet-}$ radical anion provides strong support to our conclusion that the photocurrents reported in Figure 3 are due to the photoactivity of TCNQ, and not to that of the photocatalyst particle films assembled at the ITIES.^[39] This implies that, for practical applications of photo-assisted electron transfer across ITIES (e.g., for oxidation of water to O_2) either an

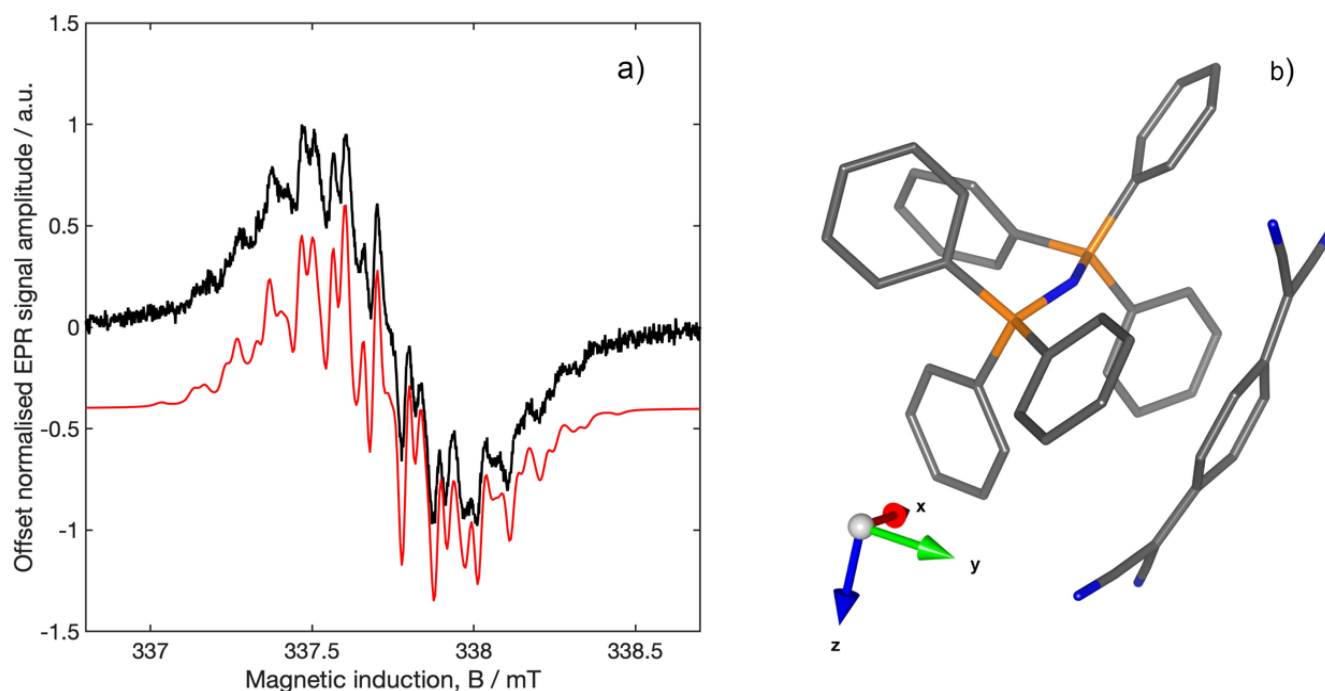


Figure 6. a) Experimental (black trace) and simulated (red trace) EPR spectra of $\text{TCNQ}^{\bullet-}$ recorded from the organic side of the ITIES between an aqueous 10 mM LiCl (pH = 11) solution and a 1 mM TCNQ + 10 mM BTPPATPBCl solution in DCE during irradiation with unfiltered light from a tungsten lamp. b) Proposed stabilisation of $\text{TCNQ}^{\bullet-}$ by formation of an adduct with BTPPA^+ . In the stick molecular model, carbon atoms are represented in grey, nitrogen atoms in blue, and phosphorus atoms in orange. Hydrogen atoms are omitted for clarity purposes.

alternative to TCNQ to be used as an electron scavenger in the organic phase is needed, or a supporting electrolyte which does not add stability to the $\text{TCNQ}^{\bullet-}$ radical anion by interaction with the electrolyte cation should be used. Please note that, although when interfacial potential differences $\Delta\phi_0^w < 0.16$ V are applied across the ITIES, TCNQ can capture an electron from the aqueous phase (see Figure 3 and corresponding discussion), this will not prevent the reaction of photoexcited TCNQ with the components of the organic electrolyte, and will still result in the degradation of the latter.

TPBCl⁻ is known to be relatively prone to oxidative degradation, and is often replaced by its tetrafluorinated analogue, tetrakis(4-fluorophenyl)borate (TPBF),^[33] which is more resistant to oxidative decomposition. For this reason, we expect the oxidation of TPBCl⁻ by photoexcited TCNQ to be the responsible of the photodegradation of the organic electrolyte. However, the TBPCl[•] radical must be rather unstable and no EPR line corresponding to species resulting from the oxidation of TPBCl⁻ or DCE was detected by EPR. According to Kotov and Kuzmin,^[44,45] the final products of the oxidation of the tetraphenylborate anion (BPh_4^-), the analogous to TBPCl⁻ used by them as the anion in the organic electrolyte, are several phenylboronates (Ph_2BO^- , PhBO_2^{2-} , PhBOH^-), of which they could detect Ph_2BO^- , PhBO_2^{2-} . By analogy, we suggest that the products of the oxidation of TBPCl⁻ are the corresponding 4-chlorophenylboronates.

Conclusions

Photo-assisted electron transfer across ITIES using simulated solar irradiation was evaluated under different conditions. A diffusion-controlled photocurrent was observed both in the presence and absence of a layer of photocatalyst particles assembled at the ITIES whenever TCNQ was present in the DCE-based organic phase. These photocurrents were, therefore, the result of the photoexcitation of the electron scavenger (TCNQ) and its reduction to the $\text{TCNQ}^{\bullet-}$ radical anion either by species present in the electrolyte (most likely the electrolyte anion, TPBCl⁻) or by an electron transferred from the aqueous phase (most likely resulting in the oxidation of H₂O). The resulting $\text{TCNQ}^{\bullet-}$ radical anion was detected using EPR, but its formation is only possible when both TCNQ and BTPPATPBCl are dissolved in DCE. The superhyperfine structure of its EPR spectrum could be reproduced by considering the interaction of the unpaired electron of $\text{TCNQ}^{\bullet-}$ with a ¹⁴N nucleus of BTPPA⁺ suggesting that the radical anion is stabilised by interaction with BTPPA⁺ in the organic phase.

These results suggest that, for practical applications of ITIES for photo-induced electron transfer from the aqueous to the organic side of the interface using solar light, a careful selection of the electron scavenger and the electrolyte used in the organic phase is needed to avoid the photo-induced degradation of the electrolyte.

Experimental Section

Reagents

Photocatalyst nanoparticles of WO_3 (< 100 nm) were obtained from Merck. TiO_2 (> 99%, 5 nm anatase) was purchased from GetNanomaterials. Aqueous solutions were prepared in deionised water (Milli-Q, $18.2 \text{ M}\Omega\text{cm}^{-1}$). 1,2-Dichloroethane (Merck, > 99.88%) was used as a solvent for the organic phase. The supporting electrolyte of the organic phase, bis(triphenylphosphoranylidene) ammonium tetrakis(4-chlorophenyl)borate ($\text{BTPPA}^+\text{TPBCl}^-$), was prepared by double substitution reaction between bis(triphenylphosphoranylidene) ammonium chloride ($\text{BTPPA}-\text{Cl}$, Merck, > 98%) and potassium tetrakis(4-chlorophenyl)borate ($\text{K}-\text{TPBCl}$, Merck, > 98%) in a 2:1 methanol: water solution and recrystallised in acetone, following the process described by D. Fermin *et al.*^[39]

Electrochemical ITIES Characterisation

The electrochemical experiments were performed within a Faraday cage, and the cell was connected using a 4-electrode arrangement to an IVIUMstat-CompactStat potentiostat. The electrochemical cell consisted of a three-compartment, all-glass cell. The Galvani potential difference at the ITIES was controlled with two Ag/AgCl (KCl_{sat}) reference electrodes placed in separate compartments connected to the main compartment by Luggin capillaries. The counter electrodes consisted of two Pt wires each placed in one of the phases of the main compartment.

ITIES between organic and aqueous-based solutions were formed in the main compartment. The geometric area of the liquid-liquid interface was 1.54 cm^2 . The organic phase solution consisted of 10 mM of $\text{BTPPA}^+\text{TPBCl}^-$ and 1 mM of 7,7,8,8-Tetracyanoquinodimethane (TCNQ) in 1,2-dichloroethane (DCE). And the aqueous phase consisted of a 10 mM LiCl solution. The pH of the solution was adjusted by dropwise addition of NaOH 1 M.

Deposition of photocatalyst nanoparticles in the ITIES was performed by dispersion of photocatalyst nanoparticles in the organic phase solution by 30 min of sonication. After sonication, the organic phase was poured into the cell, and the aqueous phase was poured on top. A subsequent sonication of 5 minutes was performed on the system to ensure the photocatalyst nanoparticles migrated to the ITIES. The system was then allowed to stabilise under darkness for 12 h.^[42]

Photoelectrocatalytic Test

In the photoelectrocatalytic tests, a four-electrode cell was used, as described in the previous section (see electrochemical ITIES characterisation). The cell was irradiated from the top using a Sciencetech solar simulator equipped with a 500 W Arc Xenon lamp and 1.5D filter featuring a manually controlled shutter. The system was allowed to reach equilibrium for 100 seconds prior to irradiating the cell. The shutter of the lamp was manually operated; hence, a 1 s offset was typically obtained.

Electron Paramagnetic Resonance (EPR) Test

EPR experiments were carried out using a Bruker EMX X-band spectrometer. A microwave frequency of 9.88 GHz and a power of 2.005 mW were used, maintaining a modulation frequency of 100 kHz and a modulation amplitude of 1 G (unless specified). All experiments were recorded at room temperature. Simulated solar light from an OSRAM Ultra Vitalux 300 W lamp was used as a source

of irradiation for the photo-induced radical production experiments.

EPR spectra of the organic phase used in the photoelectrochemical experiments at the ITIES were recorded in an ordinary 3 mm diameter Suprasil quartz EPR tube. The identification of photo-produced radicals in the organic solution was performed under different conditions. Separately, solutions of a) 1 mM TCNQ in DCE, b) solvent only (DCE), c) 10 mM $\text{BTPPA}^+\text{TPBCl}^-$ in DCE and d) 1 mM TCNQ + 10 mM $\text{BTPPA}^+\text{TPBCl}^-$ in DCE were placed in a traditional 3 mm Quartz EPR Sample tube. An EPR spectra of each sample was obtained before and after irradiation.

EPR of the organic phase at the ITIES under and after irradiation was performed in a typical EPR flat-cell Figure S4. Where the ITIES was formed by first filling the organic solution (1 mM TCNQ + 10 mM $\text{BTPPA}^+\text{TPBCl}^-$ in 1,2-DCE) through the bottom of the cell and then the aqueous solution (10 mM LiCl, pH = 11) was added dropwise over the organic phase. A similar system was described by Webster *et al.*^[50] and Dryfe *et al.*^[51] The ITIES created in the flat cell was adjusted in the cavity in such a way that the detected radicals were part of the organic solution in a region close to the interface.

Acknowledgements

EA thanks the University of Aberdeen and Curtin University for a PhD scholarship within the Aberdeen-Curtin Alliance. EA and AC acknowledge the support of the University of Aberdeen through the allocation of Pump-Priming Research and Research Networks funds.

Conflict of Interests

The authors declare no conflict of interest.

Data Availability Statement

The data that support the findings of this study are available from the corresponding author upon reasonable request.

Keywords: Photocatalysis · ITIES · Photochemistry · EPR · TCNQ

- [1] F. Dawood, M. Anda, G. M. Shafiullah, *Int. J. Hydrogen Energy* **2020**, *45*, 3847–3869.
- [2] International Energy Agency, “Carbon Capture, Utilisation and Storage—Analysis - IEA,” can be found under <https://www.iea.org/reports/carbon-capture-utilisation-and-storage-2022>.
- [3] A. Fujishima, K. Honda, *Nature* **1972**, *238*, 37–38.
- [4] M. A. Hassaan, M. A. El-Nemr, M. R. Elkatory, S. Ragab, V.-C. Niculescu, A. El Nemr, *Top. Curr. Chem.* **2023**, *381*, 31.
- [5] S. A. Savant, G. De Angelis, S. Nandy, E. Amstad, S. Haussener, *Cell Rep. Phys. Sci.* **2023**, *5*, 101755.
- [6] M. Saleh, H. N. Abdelhamid, D. M. Fouad, H. M. El-Bery, *Fuel* **2023**, *354*, 129248.
- [7] H. Yu, S. Li, S. Peng, Z. Yu, F. Chen, X. Liu, J. Guo, B. Zhu, W. Huang, S. Zhang, *Int. J. Hydrogen Energy* **2023**, *48*, 975–990.
- [8] K. Hkiri, H. E. A. Mohamed, N. Harrisankar, A. Gibaud, E. van Steen, M. Maaza, *Catal. Commun.* **2024**, *187*, 106851.
- [9] D. N. Shvalyuk, M. G. Shelyapina, I. A. Zvereva, *Results Chem.* **2023**, *7*, 101296.

- [10] J. Ran, J. Yu, M. Jaroniec, *Green Chem.* **2011**, *13*, 2708–2713.
- [11] H. Khan, M. U. H. Shah, *J. Environ. Chem. Eng.* **2023**, *11*, 111532.
- [12] A. A. Ismail, D. W. Bahnemann, *J. Phys. Chem. C* **2011**, *115*, 5784–5791.
- [13] X. Wang, K. Zhang, X. Guo, G. Shen, J. Xiang, *New J. Chem.* **2014**, *38*, 6139–6146.
- [14] T. Umebayashi, T. Yamaki, H. Itoh, K. Asai, *J. Phys. Chem. Solids* **2002**, *63*, 1909–1920.
- [15] D. Y. C. Leung, X. Fu, C. Wang, M. Ni, M. K. H. Leung, X. Wang, X. Fu, *ChemSusChem* **2010**, *3*, 681–694.
- [16] K. Woan, G. Pyrgiotakis, W. Sigmund, *Adv. Mater.* **2009**, *21*, 2233–2239.
- [17] A. Fuerte, M. D. Hernández-Alonso, A. J. Maira, A. Martínez-Arias, M. Fernández-García, J. C. Conesa, J. Soría, *Chem. Commun.* **2001**, *1*, 2718–2719.
- [18] S. Yu, H. J. Yun, D. M. Lee, J. Yi, *J. Mater. Chem.* **2012**, *22*, 12629–12635.
- [19] R. Li, *Chin. J. Catal.* **2017**, *38*, 5–12.
- [20] M. Zhan, M. Fang, L. Li, Y. Zhao, B. Yang, X. Min, P. Du, Y. Liu, X. Wu, Z. Huang, *Mater. Sci. Semicond. Process* **2023**, *166*, 107697.
- [21] P. Peljo, H. H. Girault, Liquid/Liquid Interfaces, Electrochemistry at Update based on the original article by Frédéric Reymond, Hubert H. Girault, Encyclopedia of Analytical Chemistry, © 2000, John Wiley & Sons, Ltd, Encycl. Anal. Chem. **2012**. <https://doi.org/10.1002/9780470027318.a5306.pub2>.
- [22] M. D. Kandelaki, A. G. Volkov, *Can. J. Chem.* **1991**, *69*, 151–156.
- [23] M. D. Kandelaki, A. G. Volkov, V. V. Shubin, L. I. Boguslavsky, *Bioch. Biophys. Acta Bioenerg.* **1987**, *893*, 170–176.
- [24] A. G. Volkov, *Bioelectrochem. Bioenerg.* **1984**, *12*, 15–24.
- [25] M. D. Kandelaki, A. G. Volkov, A. L. Levin, L. I. Boguslavsky, *J. Electroanal. Chem.* **1983**, *156*, 167–172.
- [26] V. Marecek, A. H. De Armond, M. K. De Armond, *J. Am. Chem. Soc.* **1989**, *111*, 2561–2564.
- [27] F. L. Thomson, L. J. Yellowlees, H. H. Girault, *Chem. Commun.* **1988**, 1547–1549.
- [28] A. R. Brown, L. J. Yellowlees, H. H. Girault, *Faraday Trans.* **1993**, *89*, 207–212.
- [29] Z. Samec, A. R. Brown, L. J. Yellowlees, H. H. Girault, K. Basě, *J. Electroanal. Chem.* **1989**, *259*, 309–313.
- [30] Z. Samec, A. R. Brown, L. J. Yellowlees, H. H. Girault, *J. Electroanal. Chem.* **1990**, *288*, 245–261.
- [31] N. Eugster, D. J. Fermín, H. H. Girault, *J. Phys. Chem. B* **2002**, *106*, 3428–3433.
- [32] N. Eugster, H. Jensen, D. J. Fermín, H. H. Girault, *J. Electroanal. Chem.* **2003**, *560*, 143–149.
- [33] H. Jensen, D. J. Fermín, H. H. Girault, *Phys. Chem. Chem. Phys.* **2001**, *3*, 2503–2508.
- [34] H. Jensen, J. J. Kakkassery, H. Nagatani, D. J. Fermín, H. H. Girault, *J. Am. Chem. Soc.* **2000**, *122*, 10943–10948.
- [35] D. J. Fermín, H. Dung Duong, Z. Ding, F. Brevet, H. H. Girault, *Phys. Chem. Chem. Phys.* **1999**, *1*, 1461–1467.
- [36] D. J. Fermín, H. D. Duong, Z. Ding, P. F. Brevet, H. H. Girault, *J. Am. Chem. Soc.* **1999**, *121*, 10203–10210.
- [37] D. J. Fermín, Z. Ding, H. D. Duong, P. F. Brevet, H. H. Girault, *J. Phys. Chem. B* **1998**, *102*, 10334–10341.
- [38] H. Jensen, D. J. Fermín, J. E. Moser, H. H. Girault, *J. Phys. Chem. B* **2002**, *106*, 10908–10914.
- [39] B. Su, D. J. Fermín, J. P. Abid, N. Eugster, H. H. Girault, *J. Electroanal. Chem.* **2005**, *583*, 241–247.
- [40] D. J. Fermín, H. Jensen, J. E. Moser, H. H. Girault, *ChemPhysChem* **2003**, *4*, 85–89.
- [41] D. Plana, D. J. Fermín, *J. Electroanal. Chem.* **2016**, *780*, 373–378.
- [42] D. Plana, K. A. Bradley, D. Tiwari, D. J. Fermín, *Phys. Chem. Chem. Phys.* **2016**, *18*, 12428–12433.
- [43] V. Dutta, S. Sharma, P. Raizada, V. K. Thakur, A. A. P. Khan, V. Saini, A. M. Asiri, P. Singh, *J. Environ. Chem. Eng.* **2021**, *9*, 105018.
- [44] N. A. Kotov, M. G. Kuzmin, *J. Electroanal. Chem.* **1990**, *285*, 223–240.
- [45] N. A. Kotov, M. G. Kuzmin, *J. Electroanal. Chem.* **1992**, *338*, 99–124.
- [46] R. S. Vishwanath, E. Witkowska Nery, M. Jönsson-Niedziółka, *J. Electroanal. Chem.* **2019**, *854*, 113558.
- [47] O. G. Khvostenko, R. R. Kinzyabulatov, L. Z. Khatymova, E. E. Tseplin, *J. Phys. Chem. A* **2017**, *121*, 7349–7355.
- [48] P. H. H. Fischer, C. A. McDowell, *J. Am. Chem. Soc.* **1963**, *85*, 2694–2696.
- [49] P. H. Rieger, I. Bernal, W. H. Reinmuth, G. K. Fraenkel, *J. Am. Chem. Soc.* **1963**, *85*, 683–693.
- [50] R. D. Webster, R. A. W. Dryfe, B. A. Coles, R. G. Compton, *Anal. Chem.* **1998**, *70*, 792–800.
- [51] R. A. W. Dryfe, R. D. Webster, B. A. Coles, R. G. Compton, *Chem. Commun.* **1997**, 779, 779–780.

Manuscript received: April 27, 2024

Revised manuscript received: July 16, 2024

Version of record online: ■ ■ ■ ■ ■

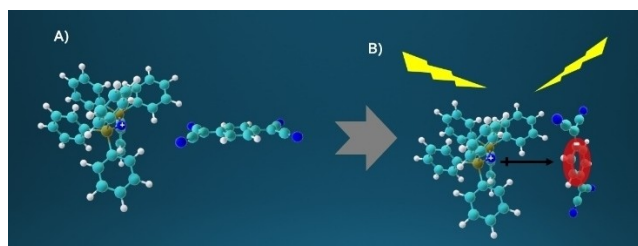


Photo-induced degradation of the organic phase was observed under solar light irradiation of the interface between two immiscible electrolytes in the presence of the electron scavenger 7,7',8,8'-Tetracyanoquinimethane (TCNQ). EPR spectroscopy demonstrated the interaction of photoexcited TCNQ with the supporting

electrolyte, bis(triphenylphosphoranylidene) ammonium tetrakis(4-chlorophenyl)borate (BTPPA⁺TPBCl⁻), favoured by the stabilisation of the resulting TCNQ^{•-} anion radical through the formation of the adduct [BTPPA⁺-TCNQ^{•-}].

*E. Avella, A. Folli, A. Cuesta**

1 – 9

Inhibition of Photocatalyst-Assisted Electron Transfer at ITIES Under Simulated Solar Irradiation—the Role of Supporting Electrolyte

